Ferromagnetic Behavior and Its Dependence on the Crystal Orientation and on the Method of Demagnetization in Single Crystals and a Polycrystal of 0.5 Percent Aluminium Iron

Ferromagnetic Behavior and Its Dependence on the Crystal Orientation and on the Method of Demagnetization in Single Crystals and a Polycrystal of 0.5 Percent Aluminium Iron*

Mikio YAMAMOTO and Ryôfu MIYASAWA**

Research Institute for Iron, Steel and Other Metals

(Received September 12, 1961)

Synopsis

The magnetization curve, ballistic demagnetizing factor (as defined with respect to the break point of the descending hysteresis curve), N, domain distribution, magnetocrystalline anisotropy constants, K_1 and K_2, as well as K_0, saturation magnetic field, H_s, residual magnetization (as the magnetization at the break point of the descending hysteresis curve), I_k, coercive force, H_c, and initial magnetic susceptibility, χ_0, and their dependence on the crystal orientation have been studied at ordinary temperatures, using the ballistic method, with single crystals and a polycrystal of iron containing 0.53% Al in thermally demagnetized (TD) state and in alternating-current demagnetized (AD) state.

It has been discovered that, irrespective of either single crystal or polycrystal and of crystal orientation, $N_{TD}>N_{AD}>N_a$, where N_a is Shuddemagen's demagnetization factor. This fact suggests that the domain distributions in TD and in AD states are different in such a way that, in TD state, the volume of domains magnetized along a direction of easy magnetization far from the rod axis of the specimen is larger than that of domains magnetized along a direction of easy magnetization nearest to the rod axis, as compared with AD state. This may be interpreted by an idea that TD and AD induce additional small uniaxial magnetic anisotropies with positive and negative anisotropy constants, respectively, the former anisotropy being due to directional ordering (the self magnetic-anneal effect), and the latter due to the re-distribution of interstitial foreign atoms.

It has been found that $(K_0)_{TD}>(K_0)_{AD}$ and $(K_1)_{TD}>(K_1)_{AD}$, and that, irrespective of either single crystals or polycrystal and of crystal orientation, $A_{TD}>A_{AD}$ $(A=\int_0^{I_s} HdI)$, $(H_s)_{TD}>(H_s)_{AD}$, $(I_k)_{TD}<(I_k)_{AD}$, $(H_c)_{TD}=(H_c)_{AD}$, and $(\chi_0)_{TD}>(\chi_0)_{AD}$. It has also been found that, in single crystals, $(H_{s[110]}-H_{s[100]})_{TD}>(H_{s[110]}-H_{s[100]})_{AD}>0$, and $(H_{s[110]}-H_{s[111]})_{TD}>(H_{s[110]}-H_{s[111]})_{AD}>0$, and $(I_k)_{AD}>(I_k)_{TD}>I_s/\sum_i \beta_i$ (Kaya's rule), where β_i's $(i=1, 2, 3)$ are the direction cosines, referred to the tetragonal axes, of the rod axis of the single crystal specimen. We have found, further, that $(K_2)_{TD}<(K_2)_{AD}$, and that, irrespective of the method of demagnetization, $3/2>K_2/K_1>-3$, $H_{s[110]}>H_{s[111]}>H_{s[100]}$, $(H_s)_{poly}>(H_s)_{single}$, $(I_k)_{poly}>I_s/\sum_i \beta_i$, $H_{c[100]}<H_{c[110]}<H_{c[111]}$, $(H_c)_{poly}>(H_c)_{single}$, $\chi_{0[100]}>\chi_{0[110]}>\chi_{0[111]}$, and $(\chi_0)_{poly}>(\chi_0)_{single}$.

It is shown that the measured facts concerning the difference in the method of demagnetization may be explained by the above-mentioned idea of small uniaxial ferromagnetic anisotropies with negative and positive anisotropy constants, induced, respectively, by TD and AD, and that the observed relations between the polycrystal and single crystal data may be interpreted in terms of the magnetic interaction between crystal grains. It is also shown, for both of TD and AD states, that the observed anisotropy of H_c coincides

---

* The 1035th report of the Research Institute for Iron, Steel and Other Metals. The original of this paper, written in Japanese language, was published in Nippon Kinzoku Gakkai-shi, 25 (1961), 437, 441, 446.

** Now at the Physics Department of Hirosaki University (Hirosaki, Japan).

well with a formula $H_c=H_{c[100]}(\Sigma_i\beta_i/\Sigma_i\beta_i^3)$, which is derived from Kondorsky-Vonsovsky's theory for the case where the 180° domains are grouped and $I_k=I_s/\Sigma_i\beta_i$ (Kaya's rule) and that the observed anisotropy of χ_0 accords well with a formula $\chi_0=\chi_{0[100]}[2(\Sigma_i\beta_i^3/\Sigma_i\beta_i)-\Sigma_i\beta_i^4/(\Sigma_i\beta_i)^2]$, which are derived from Brown's theory of the domain wall displacements for the case where 180° domain are grouped and the relative volumes of domains in unmagnetized state are expressed as $v_{i0}=(1/2)(\beta_i/\Sigma_i\beta_i)$.

Furthermore, it has been found that a formula $|K_1|=aI_s(H_s)_{poly}$, where $a=1/3\sim1/4$, holds for cubic ferromagnetics.

I. Introduction

As regards the ferromagnetic behavior of single crystals of pure iron and iron-silicon alloys, numerous works[1] have already been done since Beck[2] firstly found an anisotropy in magentization curves of 1.7% Si-Fe single crystals. The results of those works include the establishment of the anisotropy in magnetization curves, the clarification of the forms of those parts of the magnetization curves which correspond to the continuous rotation of magnetization vectors, the determination of values of the remanence and coercive force characterizing the hysteresis curve, etc. Also, since Kaya and Takaki[3] showed in 1935 that the trends of magnetization curves of iron single crystals in a weak magnetic field range may differ remarkably according to the method of demagnetization, attentions have been paid to the ferromagnetic behavior in weak magnetic field and its dependence on the method of mangetization and on an externally applied stress (cf. section II).

Now, as to the magnetic properties of iron-aluminium alloy single crystals, detailed studies on the magnetization curves have not yet been made, although the ferromagnetic anisotropy constants have been determined quite recently by Gengnagel[4]. On the other hand, regarding the effect of the method of demagnetization on the ferromagnetic properties, only the ferromagnetic behavior in weak magnetic fields, in particular, the initial susceptibility and the steep portions of magnetization curves have been examined[3,5-7] mostly with iron single crystals and the behavior in strong magnetic fields and that relating to the magnetic hysteresis have never been studied, as will be mentioned in detail later in section II. In view of these, we have studied the ferromagnetic behavior and its dependence on the crystal orientation as well as on the method of demagnetization with single crystal and polycrystal rod specimens of iron containing 0.53% Al. Although it was expected that such an iron containing a small quantity of aluminium was not so

(1) Cf. R. M. Bozorth: *Ferromagnetism*, D. Van Nostland, (1951).
(2) K. Beck: Zürich Naturforsch. Ges., **63**(1918), 116. See also L. W. McKeehan: Trans. AIME, **111** (1934), 11.
(3) S. Kaya and H. Takaki: J. Fac. Sci. Hokkaido Univ., **1** (1935), 227; Sci. Rep. Tôhoku Univ., Honda Anniv. Vol., **1**(1936), 314.
(4) H. Gengnagel: Naturwiss., **44** (1958), 630.
(5) Y. Shimizu: Nippon Kinzoku Gakkai-shi: **5** (1941), 175 (in Japanese).
(6) S. Kaya, T. Taoka, and T. Iki: Proc. Phys.-Math. Soc. Japan, **24** (1942), 864.
(7) Y. Tomono: J. Phys. Soc. Japan, **4** (1949), 196.

different from pure iron in ferromagnetic behavior, the results of measurement have shown considerable differences.

II. Previous studies on the effect of the method of demagnetization on the ferromagnetic behavior

Kaya and Takaki[3] found firstly in 1935 that the ferromagnetic behavior of iron single crystals in weak magnetic field was observed differently by employing different methods of producing the initial unmagnetized state, namely by employing either the thermal demangetization (TD) or the alternating-field demagnetization(AD).* They measured magnetization curves in TD and in AD states, and showed that, for [100] crystal specimens (round-bar single crystal specimens whose rod axes are close to a [100] direction), the difference between TD and AD magnetization curves was only slight, and, for [110] crystal specimens, the AD magnetization curve was steeper than the TD one, while, for [111] crystal specimens, the reverse was true. It is to be noted, however, that their measurements did not cover the initial permeability range.

In 1941, Shimizu[5] discovered, with iron single crystals, that the TD magnetic susceptibilities, $(\chi_0)_{TD}$, (85.4, 46.8, and 39.2 for the [100], [110], and [111] directions, respectively) were several times larger than the AD susceptibilities, $(\chi_0)_{AD}$, (26.6, 18.7, and 13.9 for the [100], [110], and [111] directions, respectively), although their degrees of anisotropy were not so different from each other (see Fig. 12 (b). He also found that the anisotropy of $(\chi_0)_{AD}$ was null for the dimension ratio (length/diameter) of the crystal specimen below, 10, but it increased rapidly as the dimension ratio increases over 10, finally attaining to an approximately constant value (corresponding to the data referred above in parentheses and shown in Fig. 12 (b)) for the dimension ratio of 100, that $(\chi_0)_{AD}$ decreased exponentially as the maximum amplitude of the alternating field adopted for demagnetization increased, and that the anisotropy of $(\chi_0)_{AD}$ was dependent on the temperature in such a manner that $\chi_{0[100]} : \chi_{0[110]} : \chi_{0[111]}$ was $1 : 1/2 : 1/3$ at $-170°C$ and became $1 : 1 : 1$ just below the Curie temperature.

Kaya, Taoka, and Iki[6] confirmed that, for iron single crystals, the TD initial permeability, $(\mu_0)_{TD}(\cong 4\pi(\chi_0)_{TD})$, (578, 490, and 269 for the [100], [110], and [111] directions, respectively) was larger than the AD ones, $(\mu_0)_{AD}$, (346, 393, and 186 for the [100], [110], [111] directions, respectively). They explained this fact as follows :— μ_0 or χ_0 in iron single crystals is associated only with 180° domain wall displacements, and, by AD, the area of 180° domains increases, but the volume of individual domains also increases, resulting an increase in scattered magnetic field, which overcomes the effect of the increase in area of 180° walls.

Shimizu[5] also studied the effect of heating on $(\chi_0)_{TD}$ and $(\chi_0)_{AD}$ in iron single

* Besides of these two methods, the mechanical shaking and the reduction to zero of the applied magnetic field from a special point on the magnetic hysteresis curve can also demagnetize the specimen, but these methods are not commonly adopted because of the trouble involved in those procedures.

crystals, and found that $(\chi_0)_{TD}$ was generally higher than $(\chi_0)_{AD}$, both being equal just below the Curie temperature, although, for the [100] and [110] directions, $(\chi_0)_{TD}$ was lower than $(\chi_0)_{AD}$ at temperatures above about 550°C. According to Tomono's[7] measurements with iron single crystals, $(\mu_0)_{TD}$ (1,000, 700, and 500 for the [100], [110], and [111] directions, respectively) is higher than $(\mu_0)_{AD}$ (600, 400, and 200 for the [100], [110], and [111] directions, respectively) at ordinary temperatures, but $(\mu_0)_{AD}$ is lower than $(\mu_0)_{TD}$ at temperatures above about 400°C, both becoming equal just below the Curie temperature. Further, Shimizu[5] has shown, with polycrystalline iron, nickel, and 60 and 81.5% Ni-Fe alloys, that $(\chi_0)_{AD}$ is higher than $(\chi_0)_{TD}$ at ordinary temperatures and that, at high temperatures, the same relation holds for iron, while the relation reverses once at intermediate temperatures for nickel and nickel-iron alloys.

As seen from the above description, the previous studies on the effect of the method of demagnetization on ferromagnetic behavior are concerned mostly with iron single crystals and exclusively with weak field behavior, particularly with the initial magnetic susceptibility. We have studied at ordinary temperatures the effect of the method demagnetization not only on the initial susceptibility but also on the demagnetizing factor, domain distribution, saturation field, ferromagnetic anisotropy constants, residual magnetization, and coercive force in single crystal and polycrystal rods of iron-aluminium alloy containing 0.53% Al.

III. Specimens and experimental procedure

Single crystal specimens used are round bars, 2.3~2.7 mm in diameter and 5.7~13.3 cm in length, produced by the strain-anneal method from iron containing 0.53% Al and 0.018% C[8]. Their orientations are close to the three principal crystallographic directions [100], [110], and [111] and intermediate between [100] and [110] directions (Fig. 1). These single crystal specimens are called, for brevity, as the [100], [110], [111], and [100/110] crystal specimens hereafter. Their dimensions and orientations as determined by the light-figure method[9] are given in Table 1, in which $(\beta_1, \beta_2, \beta_3)$ are the direction cosines referred to the tetragonal crystal axes of the

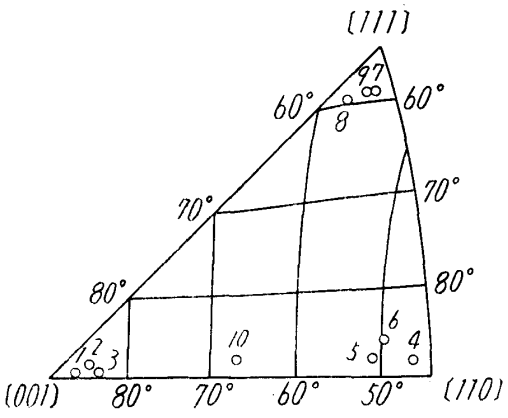

Fig. 1. Orientations of single crystal rod specimens of 0.53% aluminium iron.

(8) M. Yamamoto and R. Miyasawa: Nippon Kinzoku Gakkai-Shi, **16** (1952), 305: Sci. Rep. RITU, **A6** (1954), 333.

(9) M. Yamamoto and J. Watanabé: Nippon Kinzoku Gakkai-shi, **17** (1953), 5 and 7; Sci. Rep. RITU, **A7** (1955), 173.

rod axis. The polycrystal specimen is a round bar subjected to the decarburization treatment in the procedure of the strain-anneal method for growing single crystals.[8] Its grain size is 140 mm^{-2}. Its dimensions are also given in Table 1.

Table 1. Orientations of single crystal rod specimens, and dimensions and Shuddemagen's demagnetizing factors (N_a) of single crystal and polycrystal rod specimens, of 0.53% aluminium iron.

Specimen		Direction cosines of the rod axis referred to the crystal axes			Length	Diameter	N_a
Group	No.	β_1	β_2	β_3	cm	cm	
[100]	1	0.998	0.063	0.012	6.698	0.2269	0.0353
	2	0.995	0.090	0.033	8.312	0.2696	0.0328
	3	0.994	0.112	0.014	7.050	0.2531	0.0390
[110]	4	0.723	0.690	0.023	6.900	0.2576	0.0416
	5	0.776	0.630	0.037	6.988	0.2614	0.0419
	6	0.761	0.645	0.077	5.692	0.2302	0.0497
[111]	7	0.627	0.585	0.515	7.334	0.2544	0.0367
	8	0.667	0.548	0.504	13.330	0.2618	0.0139
	9	0.639	0.574	0.512	9.620	0.2516	0.0228
[100/110]	10	0.919	0.392	0.040	6.096	0.2566	0.0512
Polycrystal	11	Grain size 140 mm^{-2}			6.904	0.2530	0.0403

The magnetic measurements were made ballistically at room temperature using the pulling-out procedure. As the demagnetizing factors of the specimens, Shuddemagen's[10] values, N_a, were employed preliminarily, but the values, N, determined experimentally in this study were adopted later (see Section IV). The two water-jacked magnetizing solenoids were used; one of the length of 39.4 cm with the coil constant of 59.4 Oe/A and the other of the length of 49.8 cm with the coil constant of 58.5 Oe/A.

As the methods of demagnetization of the specimens, we employed the thermal method and decreasing alternating-field methods, which are called, for brevity, TD and AD, respectively, in the following. TD was done by heating the specimen at 850°C over the Curie temperature for an hour in vacuum using a non-inductively wound nichrome furnace, and AD was done by putting the specimen in the magnetizing solenoid, through which decreasing alternating magnetic field with the maximum amplitude of 300~360 Oe was passed.

IV. Magnetization curves

Firstly, the measured values of the magnetization, I, were plotted against the effective magnetic field,

(10) B. Shuddemagen: Ann. Physik, **7** (1902), 942.

$$H_a = H_{ex} - N_a I \ , \tag{1}$$

where H_{ex} is the externally applied field and N_a Shuddemagen's demagnetizing factor.[10] The weak-filed parts of the I-H_a curves for [100] (No, 1), [110] (No. 4), [111] (No. 7), and polycrystal (No. 11) specimens in TD and in AD states are shown in Fig. 2(a) and (b).

The trend of the magnetization curves of the single crystal specimens is similar to that of the curves of iron single crystals[11]; the descending hysteresis curve displays a sharp break for any crystal orientation, irrespective of the method of demagnetization. This can also be said approximately equally regarding the hysteresis curve of the polycrystal specimen. Moreover, regardless of either single crystals or polycrystal and irrespective of the method of demagnetization, the course of the descending hysteresis curve from its break point to somewhere beyond the coercive force state ($I=0$, $H=H_c$) is nearly linear. The comparison between magnetization curves measured in TD and in AD states (Fig. 2) indicates that the

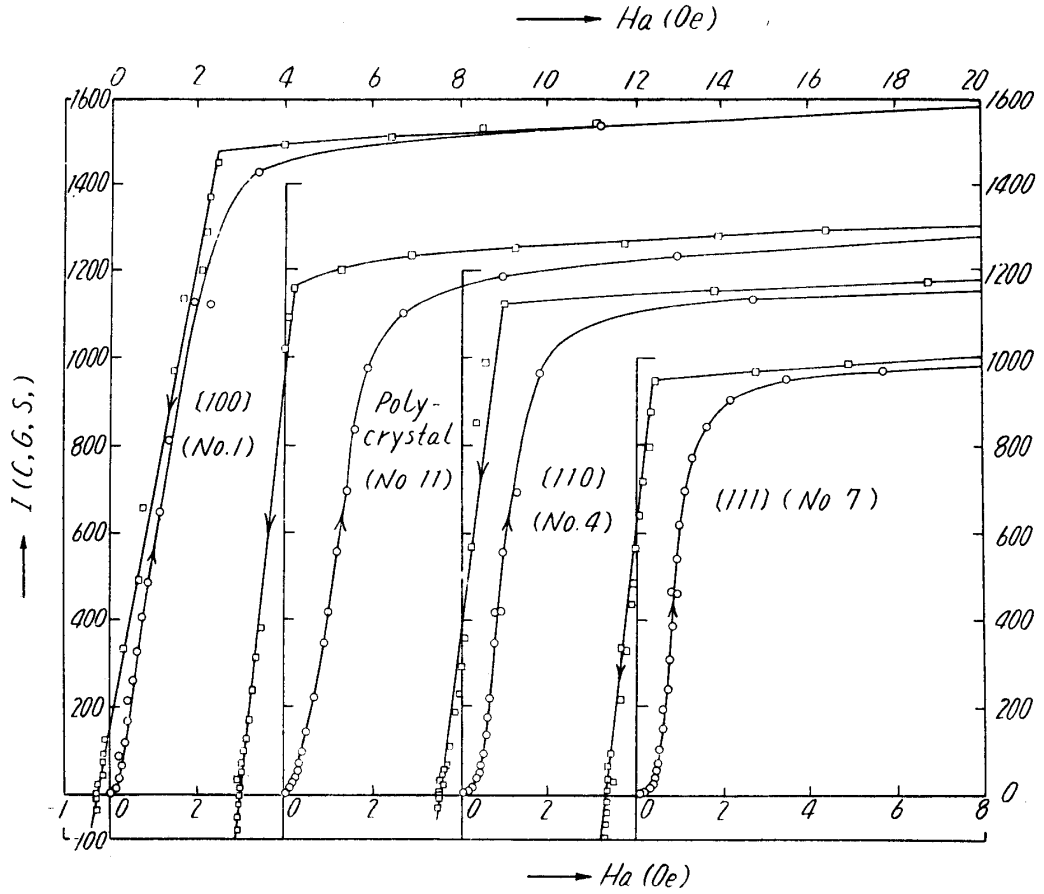

(a) TD state

Fig. 2. Magnetization curves for low fields, as plotted using Shuddemagen's demagnetizing factors, in thermally demagnetized (TD) state (a) and in alternating-current demagnetized (AD) state (b) of single crystal and polycrystal rod specimens of 0.53% aluminium iron.

(11) S. Kaya: Z. Phys., **84** (1935), 705.

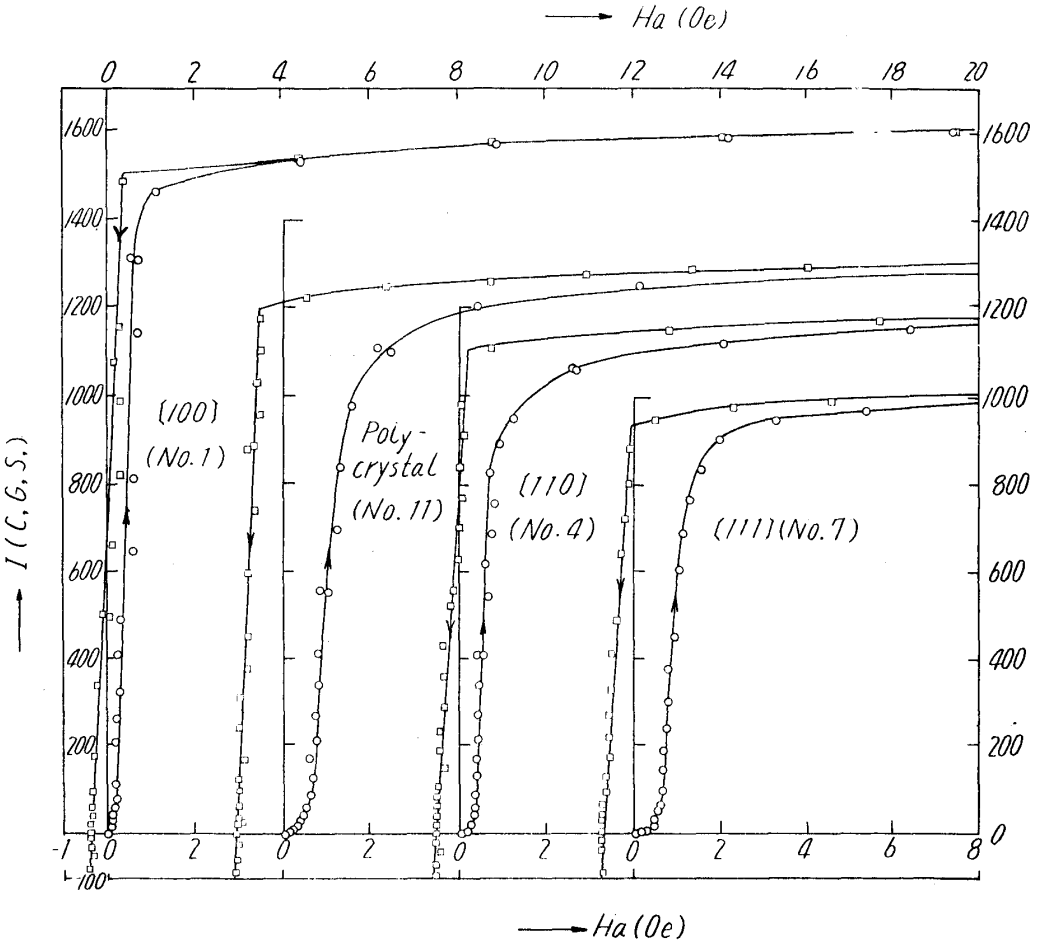

(b) AD state
Fig. 2. Continued.

AD curve is steeper than the TD one, irrespective of either single crystals or polycrystal. Particularly, in AD state, the values of the magnetic field where the break of the descending hysteresis curve locate, H_a^k, are generally close to the zero value and take positive and negative values nearly equally, while they generally are positive in TD state (cf. Table 2).

V. Physical meaning of the magnetic field where the break of the descending hysteresis curve locates

The above-mentioned break of the descending hysteresis curve is the point where the retrogression of the process of reversible rotation of magnetization vectors ends and also some of non-180° wall displacements occur, resulting the distribution of magnetization vectors according to Kaya's rule, namely in proportion to the cosines of angles which the magnetization vector makes with directions of easy magnetization nearer to the field direction.[11,12] When the mangetization is reduced further from this break point, 180° wall displacements are thought to occur exclusively, the magnetization passing through zero and then increasing in

(12) M. Yamamoto : Nippon Butsuri Gakkai-shi, **7** (1948), 91 (in Japanese).

the reverse direction.[13] Then, this break point is the critical field for the 180° wall displacement, and consequently the field where the break point locates should be negative. And, the part of the descending hysteresis curve just beyond the break point or critical field for the 180° wall displacement, where the majority of 180° wall displacements is thought to occur simultaneously, practically drops perpendicularly. Thus, the field corresponding to the break point is practically equal to the coercive force, H_c, which can be determined experimentally independently of the demagnetizing factor.

VI. Ballistic demagnetizing factor as defined in reference to the break point of the descending hysteresis curve

According to the just-mentioned consideration, the "true" effective field, H_k, corresponding to the break point of the descending hysteresis curve is given by

$$H_k = H_{ex}{}^k - NI_k = H_c \ , \tag{2}$$

where $H_{ex}{}^k$ and I_k are, respectively, the external field and magnetization corresponding to the break point, and N is the "true" demagnetizing factor. Then, the "true" demagnetizing factor, N, can be determined from

$$N = (H_{ex}{}^k - H_c)/I_k = N_a + (H_a{}^k - H_c)/I_k \ . \tag{3}$$

The values of N as determined from Eq. (3) using the values of N_a (Table 1) and measured data of $H_a{}^k$, I_k and H_c (Table 2) are given in Table 2. Irrespective of the crystal orientation and regardless of either single crystals or polycrystal, thus determined N values in TD and AD states, N_{TD} and N_{AD}, and N_a are in the following order (cf. Tables 1 and 2):

$$N_{TD} > N_{AD} > N_a \ . \tag{4}$$

Only for the [100/110] crystal (No. 10), $N_{TD}=N_{AD}>N_a$. It is to be noted, further, that the average value of $(N_{TD}-N_{AD})/N_{AD}$ is 2%.

Fig. 3 shows the rotation parts of I-$H(=H_{ex}-NI)$ curves for TD and AD states as calculated using the N values. They may seem, at first sight, to be independent of the method of demagnetization, but, actually, the I-H curves for TD and AD states are different in detailed points, as shown later.

VII. Interpretation of the difference between the demagnetizing factors for TD and AD states

As can be seen from the above-mentioned, N_{TD} and N_{AD} are actually the ballistic demagnetizing factors, namely, demagnetizing factors for the central part of a rod specimen, as defined with respect to the break point of the descending hysteresis curve. It is well known that the demagnetizing factor, N, of a homogeneous slender rod specimen such as used here is determined mainly by the

(13) According to the reference made by S. V. Vonsovsky : J. Phys. USSR, **11** (1940), 11, E. J. Kondorsky [C.R. Acad. Sci. USSR, **18** (1938), 325] considers similarly.

Table 2. Measured data of the "apparent" effective mangetic field "ture" demangetizing factor (N), work required to field(H_s), magnetization corresponding to $H_a{}^k$ (I_k), coercive state and in alternating-current demagnetized state, of

Specimen		Thermally demagnetized state					
Group	No.	$H_a{}^k$(Oe)	N	A (10^5 erg/cm^3)	I_s	H_s(Oe)	I_k
[100]	1	2.53	0.0372	0.034	1634	175	1487
	2	1.44	0.0341	0.08	1691	100	1444
	3	0.94	0.0399	0.04	1729	300	1506
[110]	4	0.66	0.0426	1.011	1639	705	1119
	5	0.94	0.0431	0.98	1718	555	1140
	6	0.79	0.0489	1.00	1677	685	1057
[111]	7	0.41	0.0378	1.36	1680	520	949
	8	−0.17	0.0144	1.44	1641	475	934
	9	0.39	0,0240	1.34	1619	470	931
[100/110]	10	−0.26	0.0514	0.481	1700	440	1237
Polycrystal	11	0.22	0.0414	0.735	1678	755	1164

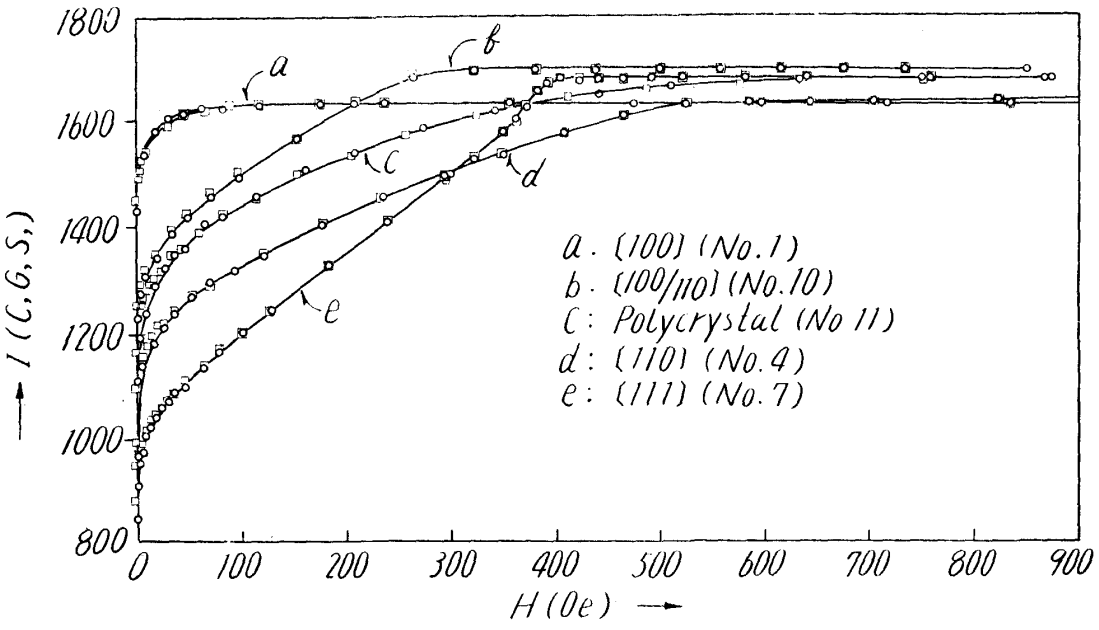

(a) TD state

Fig. 3. Magnetization curves for high fields, as plotted using "true" demagnetizing factors, in thermally demagnetized (TD) state (a) and in alternating-current demagnetized (AD) state (b) of single crystal and polycrystal rod specimens of 0.53% aluminium iron.

density of free magnetic poles distributed on its surface or the component, I_n, normal to the specimen surface of the magnetization, N being greater as I_n is larger. And, I_n is determined by the distribution of magnetic domains in the specimen in such a way that the domain distribution in which the magnetization vectors nearby the surface have larger components normal to the surface results a larger I_n. For N for the central part of the slender rod specimen, the contribu-

where the break of the descending hysteresis curve locates (H_a^k), magnetize to saturation (A), saturation magnetization (I_s), saturation force (H_c) and initial susceptibility (χ_o), in thermally demagenetized single crystal and polycrystal rod specimens of 0.53% Al-Fe alloy.

		Alternating-current demagnetized state							
H_c(Oe)	χ_o	H_a^k(Oe)	N	A (10^5 erg/cm^3)	I_s	H_s(Oe)	I_k	H_c(Oe)	χ_o
−0.29	17.6	0.39	0.0358	0.021	1628	85	1488	−0.32	13.1
−0.38	31.8	—	—	—	—	—	—	—	20.5
−0.45	34.0	—	—	—	—	—	—	—	19.0
−0.50	22.9	0.26	0.0422	0.942	1638	535	1106	−0.46	18.0
−0.49	30.8	—	—	—	—	—	—	—	17.2
−0.54	18.8	—	—	—	—	—	—	—	15.2
−0.65	26.7	0.04	0.0374	1.36	1683	425	936	−0.67	12.0
−0.67	13.6	—	—	—	—	—	—	—	6.3
−0.70	19.2	—	—	—	—	—	—	—	13.5
−0.55	22.0	−0.19	0.0514	0.454	1701	355	1237	−0.52	16.1
−1.04	59.2	−0.47	0.0407	0.679	1688	690	1197	−0.99	32.8

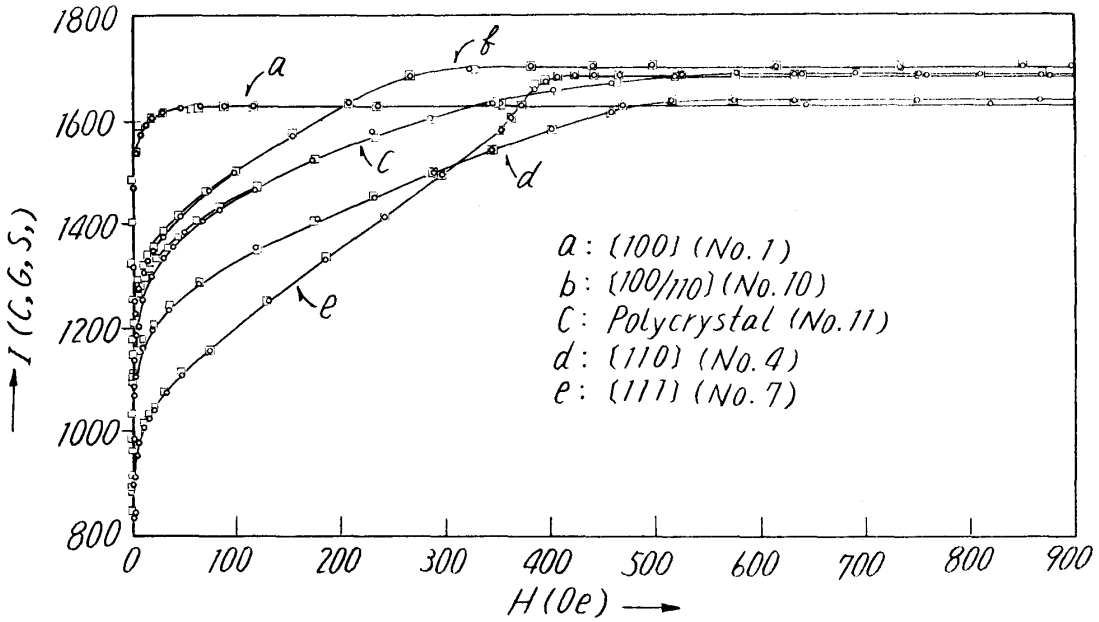

Fig. (b) AD state

Fig. 3. Continued.

tion from I_n on the end surfaces of the specimen is very small as compared to that from I_n on the side or lateral surface so that we may neglect the former contribution. Then $N_{TD}>N_{AD}$ means that the domain distribution at the break point of the descending hysteresis curve is different in TD and in AD states and magnetization vectors have larger components normal to the side surface in TD state than in AD state. It is certain that, at the break point of the descending hysteresis curve, magnetization vectors distribute along directions of easy magnetization nearer to the direction of an applied field, namely, of the rod axis. Thus, it follows that, in TD state, at the break point of the descending hysteresis curve, the volume of

domains with magnetization vectors pointing to a direction of easy magnetization far from the rod axis is larger than that of domains with magnetization vectors pointing to a direction of easy magnetization nearest to the rod axis as compared with AD state.

Now, if only the cubic magnetocrystalline anisotropy energy is present, magnetization vectors at the break point of the descending hysteresis curve distribute along directions of easy magnetization nearer to the direction of an applied field in proportion to the cosines of angles which those directions of easy magnetization make with the field direction (Kaya's rule)[11,12] and this domain distribution is thought to be independent of whether the starting unmagnetized state is TD state or AD state. But, according to the above-mentioned experimental results and interpretation of them, the domain distributions at the break point of the descending hsysteresis curve differs in TD and AD states, and, as shown later (section X), it deviates from Kaya's rule irrespective of whether the unmagnetized state is TD or AD state. Consequently, it naturally follows that domain distributions in TD and in AD state and their changes with magnetization differ from each other, too. What is the origin of such a fact ?

As just mentioned, the domain distribution obeying Kaya's rule at the break point of the descending hysteresis curve is realized when there is only the magnetocrystalline anisotropy energy proper to the substance, namely, the cubic magnetic anisotropy energy, E_c, in the case of 0.53% Al-Fe alloy concerned in this study. Consequently, it must be considered that any deviation from this domain distribution is originated from an additional existence of a uniaxial magnetic anisotropy energy, E_u, besides of E_c.

The uniaxial magnetic anisotropy energy, $(E_u)_{TD}$, which may be considered here to be induced by TD is the one originated from directional ordering which generally occurs in the magnetic-field-cooling effect in ferromagnetic cubic solid solution alloys.[14] Since this uniaxial anisotropy is induced according to the domain distribution taken at temperatures below the Curie temperature, it differs from position to position in the specimen and the direction of easy magnetization of $(E_u)_{TD}$ at a certain position coincides with the direction taken by the magnetization vector at that position on the way of cooling from alone the Curie temperatare, which is one of the directions of easy magnetization $\langle 100 \rangle$ of E_c at that position.

When the specimen in TD state is subjected to AD, a part of magnetization vectors directed formerly to $\langle 100 \rangle$ directions far from the rod axis is directed to the $\langle 100 \rangle$ direction nearest to the rod axis by an alternating magnetic field applied along the rod axis, and then intertsitial impurity atoms such as carbon, nitrogen, etc. change their occupation sites according to this domain distribution, which is thus stabilized. Consequently, the volume of domains of which the magnetization vectors are directed along the $\langle 100 \rangle$ direction nearest to the rod axis is larger

(14) S. Taniguchi and M. Yamamoto : Sci. Rep. RITU, **6** (1954), 330. S. Taniguchi : Sci. Rep. RITU, **7** (1955), 269. L. Néel : J. phys. rad., **15** (1954), 225 ; Compt. rend., **241** (1955), 533.

in AD state than in TD state. Thus, it may be thought that, by AD, a uniaxial anisotropy energy, $(E_u)_{AD}$ of which the direction of easy magnetization is the $\langle 100 \rangle$ direction nearest to the rod axis additionally induced almost uniformly over the entire of the specimen.

In short, the total ferromagnetic anisotropy energy in TD and in AD states, E_{TD} and E_{AD}, are expressed, respectively; by

$$E_{TD} = E_c + (E_u)_{TD}$$

and

$$E_{AD} = E_c + (E_u)_{TD} + (E_u)_{AD} \ . \tag{5}$$

As stated above, the directions of easy magnetization of E_c, $(E_u)_{AD}$, and $(E_u)_{TD}$ are commonly $\langle 100 \rangle$ directions, but E_c and $(E_u)_{AD}$ are homogeneous, while $(E_u)_{TD}$ is heterogeneous. Taking the average over the entire of the specimens, $(E_u)_{TD}$ is equivalent to E_u with a positive constant, while $(E_u)_{AD}$ is equivalent to E_u with a negative constant. Also, as seen from the mutual comparison of magnetization curves in Fig. 3, the magnitudes of $(E_u)_{TD}$ and $(E_u)_{AD}$ are very small as compared with that of E_c, so that practically E_{TD} and E_{AD} are only slightly modified from E_c. Thus, all of E_c, E_{TD}, and E_{AD} can be expressed commonly as

$$E = K_0 + K_1 (\alpha_1^2 \alpha_2^2 + \alpha_2^2 \alpha_3^2 + \alpha_3^2 \alpha_1^2) + K_2 \alpha_1^2 \alpha_2^2 \alpha_3^2, \quad K_1 > 0 \ , \tag{6}$$

where $(\alpha_1, \alpha_2, \alpha_3)$ are the direction cosines of the magnetization vector referred to the crystal axes, and it can be expected that

$$(K_0)_{TD} > (K_0)_{AD} \simeq K_0 \tag{7}$$

and

$$(K_1)_{TD} > (K_1)_{AD} \simeq K_1 \ . \tag{8}$$

VIII. Ferromagnetic anisotropy constants

We determined values of $\int_0^{I_s} H dI$ $(=A)$, using a planimeter, from magnetization curves (I-H curves) as plotted by adopting "true" ballistic demagnetizing factors, N, (defined referred to the break point of the descending hysteresis curve) (cf. Fig. 3). The values of A thus determined are shown in Table 2. Since, as stated above (Section VII), the ferromagnetic anisotropy energies in single crystal and polycrystal specimens of 0.53% Al-Fe alloy in TD and in AD states can practically be expressed by Eq. (6), we have, for a single crystal rod,

$$A = K_0 + K_1 \sum_{j>i} \beta_i^2 \beta_j^2 + K_2 \beta_1^2 \beta_2^2 \beta_3^2 \ , \tag{9}$$

where $(\beta_1, \beta_2, \beta_3)$ are the direction cosines of the rod referred to the crystal axes and

$$\sum_{j>i} \beta_i^2 \beta_j^2 = \beta_1^2 \beta_2^2 + \beta_2^2 \beta_3^2 + \beta_3^2 \beta_1^2 \ .$$

Thus, we can determine values of K_0 and anisotropy constant, K_1 and K_2, from Eq. (9) using the measured values of A (Table 2) and of $(\beta_1, \beta_2, \beta_3)$ (Table 1). The

Table 3. Measured values of K_0 and of the first and second cubic magnetic anisotropy constants, K_1 and K_2, and the computed values of A $(=\int_0^{I_s} HdI)$ for a polycrystal specimen, in thermally demagnetized (TD) state and in alternating-current demagnetized (AD) state, of 0.53% aluminium iron.

Demagnetized state	K_i (10^5 erg/cm^3)			A_{poly} (10^5 erg/cm^3) calculated from	
	K_0	K_1	K_2	Eq. (13)	Eq. (13a)
TD	0.018	3.99	0.78	0.823	0.798
AD	0.006	3.76	3.36	0.790	0.738

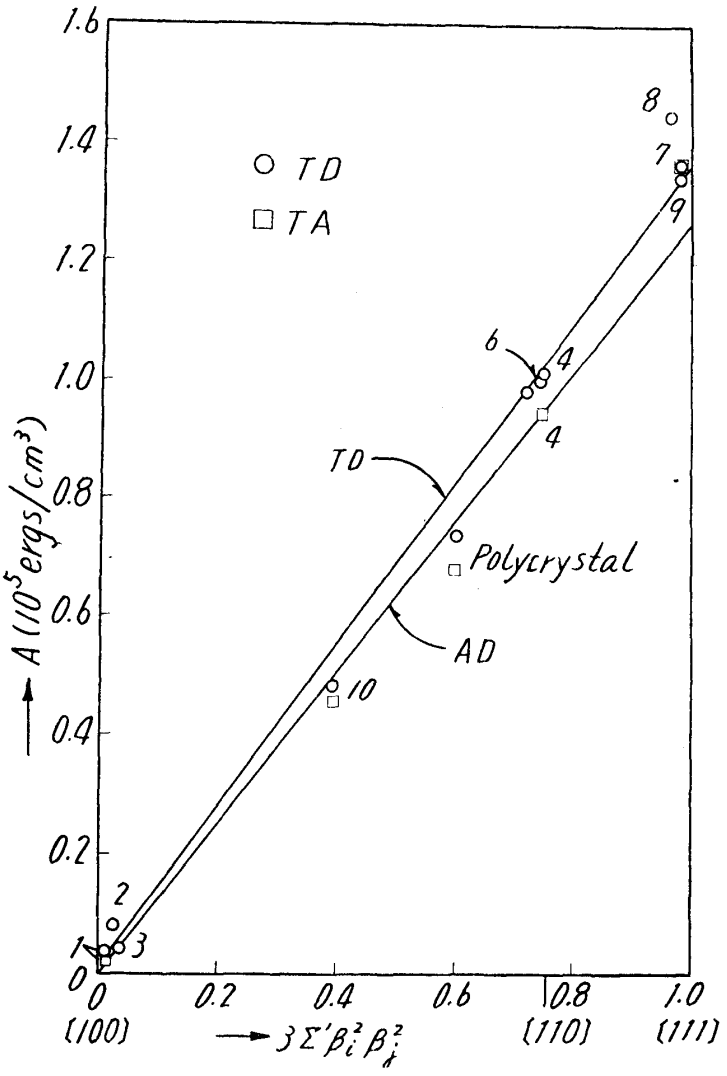

Fig. 4. Orientational dependence of A $(=\int_0^{I_s} HdI)$ in thermally demagnetized (TD) state and in alternating-current demagnetized (AD) state of 0.53% Al-Fe single crystals.

values of K_0, K_1, and K_2 determined in this way are shown in Table 3.

If the K_2 term in Eq. (9) is neglected since its orientation factor is small to the first power of ten as compared with that of the K_1 term, then it follows that A for single crystals is linear against $\sum_{j>i} \beta_i^2 \beta_j^2$. In fact, this holds here, as seen from Fig. 4 (only the measured value for the [100/110] crystal (No 10) deviates lower from linearity).

As stated before in Section VII, it is supposed that, in TD state, a uniaxial ferromagnetic anisotropy energy with a positive constant is induced according to the domain distribution taken during cooling through the Curie temperature, while, in AD state, another uniaxial anisotropy energy with the direction of easy magnetization along a $\langle 100 \rangle$ direction nearest to the rod axis of the specimen is induced additionally, the volume of domains magnetized along this $\langle 100 \rangle$ direction being larger in AD state than in TD state. Then, it can be expected that the energy required to magnetize to saturation the specimen is larger in TD state than in AD state, or

$$A_{TD} > A_{AD} \ . \tag{10}$$

In fact, as seen from Table 2, as well as from Fig. 4, this relation holds generally, irrespective of either single crystals or polycrystal (only for a [111] crystal (No. 7), $A_{TD}=A_{AD}$).

According to Table 3 and Fig. 4, $K_0(=A_{[100]})$ is practically zero irrespective of either in TD state or in AD state, but, nevertheless, the relation (7), namely $(K_0)_{TD} > (K_0)_{AD}$ as expected from the consideration in Section VII holds. Also, $(K_1)_{TD}$ is somewhat larger than $(K_1)_{AD}$ corresponding with the relation (8) deduced also from the consideration in that section. In contrary to these, $(K_2)_{TD}$ is much smaller than $(K_2)_{AD}$, namely

$$(K_2)_{TD} < (K_2)_{AD} \ . \tag{11}$$

This fact seems to be not simply interpreted. It is to be noted, further, that, regardless of either in TD state or in AD state, the following relation holds among K_1 and K_2 :—

$$3/2 > K_2/K_1 > -3 \ . \tag{12}$$

For a pseudo-isotropic polycrystal, we obtain, by averaging Eq. (9) simply over all possible orientations,

$$A_{poly} = K_0 + (K_1/5) + (K_2/105) \ , \tag{13}$$

which may be reduced to

$$A_{poly} \simeq K_1/5 \ , \tag{13a}$$

since K_0 is very small, as shown above, and the numerical factor of the K_2 term is also small. Values of A_{poly} computed from Eqs. (13) and (13a) using the measured values of K_0, K_1, and K_2 (Table 3) are given in Table 3. The comparison of these computed A_{poly} values with the values measured on the polycrystal specimen

given in Table 2 indicates that the values computed from Eq. (13) are more than 10% larger, and even those computed from (13a) are 8% larger, than the measured ones, which are also seen readily from Fig. 4. The cause for such discrepancies may be the magnetic interaction between crystal grains which has not been taken into consideration for the calculation of A_{poly} values. Thus, this effect produces free magnetic poles on grain boundaries, which are inclined to be reduced by the small rotation of magnetization vectors near the grain boundaries, so that the work of magnetization may be reduced from that in the case where this effect does not exist.

Further, one of the present authors (Yamamoto)[15] previously showed that, for cubic ferromagnetics, the magnitude of the first ferromagnetic anisotropy constant, K_1, is given practically by a quater of the product of the saturation magnetization, I_s, and the saturation field of pseudo-isotropic polycrystal, $(H_s)_{poly}$:-

$$|K_1| = I_s (H_s)_{poly}/4 \ . \tag{14}$$

But, the values of K_1 computed from Eq. (14) using the measured values of I_s and $(H_s)_{poly}$ four our polycrystal specimen of 0.53% aluminium iron given in Table 2 are 20~30% lower than the measured data. Rather,

$$|K_1| = I_s (H_s)_{poly}/3 \tag{15}$$

gives values only several percent larger than the measured values. Thus, it can be said that

$$|K_1| = \alpha I_s (H_s)_{poly}, \ \alpha = 1/3 \sim 1/4 \tag{16}$$

holds well for cubic ferromagnetics.

IX. Saturation magnetization and saturation field

Values of the saturation magnetization I_s, as determined directly from the measured magnetization curves are given in Table 2. They differ to a considerable degree from specimen to specimen, which may be ascribed mainly to the difference in aluminium content in individual specimens.

Theoretically, the saturation field, H_s, is finite only for the three principal directions of single crystal (cf. Eq. (21) given later) and is infinite for general directions in single crystal and for polycrystal. But, practically for general crystal orientations and for polycrystal, the approach of the magnetization to saturation is very slow (see Fig. 3), so that H_s is finite in the limit of accuracy in the common ballistic measurement of the magnetization curve such as adopted in the present study. The values of H_s in this sense as determined from I-H curves (cf. Fig. 3) are given in Table 2 and plotted, only for convenience, against $\sum_{i>j} \beta_i^2 \beta_j^2$

(15) M. Yamamoto : Nippon Kinzoku Gakkai-shi, **11** (1947), No. 11–12 ; **13** (1949), No. 6 ; Sci. Rep. RITU **A4** (1952), 14 (Ni-Co alloys). M. Yamamoto and S. Taniguchi: Nippon Kinzoku Gakkai-shi, **17** (1955), 532 ; Sci. Rep. RITU, **A8** (1956), 112 (Fe-Al alloys). M. Yamamoto : Sci. Rep. RITU, **A6** (1954), 446 (Ni-Cu alloys). M. Yamamoto : J. Phys. Soc. Japan, **10** (1955), 725.

in Fig. 5. These data indicate the following facts :— Firstly, irrespective of the crystal orientation and of either single crystals or polycrystal,

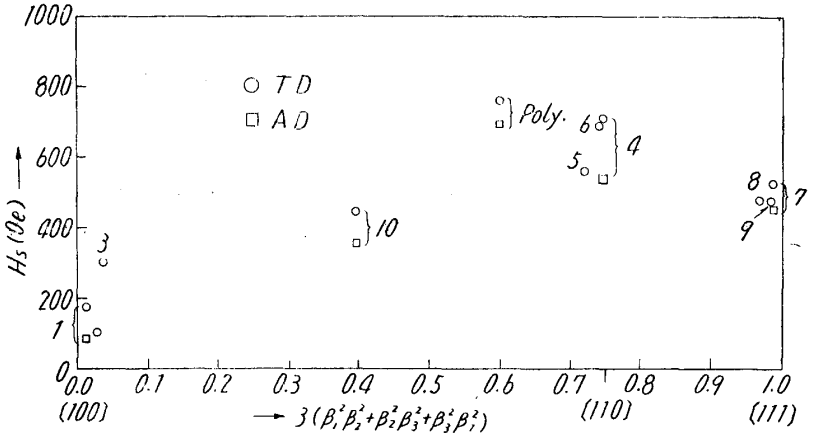

Fig. 5. Saturation magnetic field, H_s, as plotted, for convenience, against $\beta_1^2\beta_2^2+\beta_2^2\beta_3^2+\beta_3^2\beta_1^2$ (β_1,β_2 and β_3 are the direction cosines referred to the tetragonal axes of the rod axis of single crystal) in thermally demagnetized (TD) (circles) and in alternating-current demagnetized (AD) state (squares) of single crystal and polycrystal rod specimens of 0.53% aluminium iron.

$$(H_s)_{TD} > (H_s)_{AD} \ . \tag{17}$$

Secondly, for single crystals, regardless of either in TD or in AD state,

$$H_{s\,[110]} > H_{s\,[111]} > H_{s\,[100]} \ . \tag{18}$$

Thirdly, also for single crystals,

$$\left.\begin{aligned} &(H_{s\,[110]} - H_{s\,[100]})_{TD} > (H_{s\,[110]} - H_{s\,[100]})_{AD} > 0 \\ \text{and} \\ &(H_{s\,[110]} - H_{s\,[111]})_{TD} > (H_{s\,[110]} - H_{s\,[111]})_{AD} > 0 \end{aligned}\right\} \tag{19}$$

And, finally, irrespective of either in TD or in AD state,

$$(H_s)_{poly} > (H_s)_{single} \ . \tag{20}$$

The observed relation (17) is consistent with the relation (10), $A_{TD}>A_{AD}$, as found from the determination of A values in Section VIII. On the other hand, since, as mentioned before (Section VII), commonly to TD and AD states, the total magnetocrystalline anisotropy energy may be expressed practically by Eq. (6) and the directions of easy magnetization are $\langle 100 \rangle$ directions, the values of H_s for [110] and [111] directions in TD and AD states are given theoretically by the following expressions :—

$$\left.\begin{aligned} &H_{s\,[110]} = H_{s\,[100]} + 2\,(K_1/I_s) \\ \text{and} \\ &H_{s\,[111]} = H_{s\,[100]} + (4/3)\,\{(K_1 + \frac{K_2}{3})/I_s\} \ . \end{aligned}\right\} \tag{21}$$

Moreover, as stated in Section VIII, the relation (8), $(K_1)_{TD}>(K_1)_{AD}$, holds and the

relation (12), $3/2>K_2/K_1>-3$, holds irrespective of either for TD or for AD state, so that the observed relation (18) follows at once. Further, the relation (19a) follows from Eqs. (9), (21a), and (8), and the relation (19b) follows from Eqs. (19a) and (12). Finally, the observed relation (20), namely $(H_s)_{poly}>(H_s)_{single}$ regardless of the method of demagnetization, follows at once from the combination of Eqs. (16) and (21).

X. Residual magnetization as the magnetization corresponding to the break point of the descending hysteresis curve

According to the considerations in Section VII, in TD state, a uniaxial ferromagnetic anisotropy energy with a positive constant is induced according to the domain distribution taken during cooling through the Curie temperature, while, in AD state, another uniaxial anisotropy energy with a negative constant is induced. Consequently, the domain distributions at the break points of the descending hysteresis curves in TD and in AD states should deviate commonly from Kaya's rule[11,12] in such a manner that, in TD state, the volumes of domains mangetized along $\langle 100\rangle$ directions far from the rod axis are larger than those of domains mangetized along $\langle 100\rangle$ directions nearest to the rod axis as compared with AD state. It follows, then, that the magnetization at this point, I_k, is smaller in TD state than in AD state, or

$$(I_k)_{TD} < (I_k)_{AD} \ , \tag{22}$$

and that both of $(I_k)_{TD}$ and $(I_k)_{AD}$ does not strictly obey Kaya's rule

$$I_k = I_s/\sum_{i=1}^{3}\beta_i \ . \tag{23}$$

The value of I_k was determined graphically as the magnetization corresponding to the point of intersection of the slowly descending portion and the rapidly falling straight portion of the descending hysteresis curve. Thus determined I_k values are given in Table 2 and Fig. 6. But, the real determination of the I_k values was not made so accurately owing to the lack of the measured points in the slowly descending portion of the curve. Probably because of this, the effect of the method of demagnetization is not unique, as seen from Table 2 and Fig. 6. Nevertheless, the relation (22) holds for the polycrystal specimen. For single crystal specimens, irrespective of either in TD state or in AD state, the measured I_k value is a little lower than the values computed from Eq. (23) for any direction, as seen clearly from Fig. 6. Thus, we have, for single crystals.

$$(I_k)_{TD} \sim (I_k)_{AD} < I_s/\sum_{i=1}^{3}\beta_i \ . \tag{24}$$

This means that, at the break points of the descending hysteresis curves in TD and in AD states, the volumes of domains magnetized along the directions of easy magnetization far from the rod axis are commonly larger than those of domains magnetized along the directions of easy magnetization near to the rod

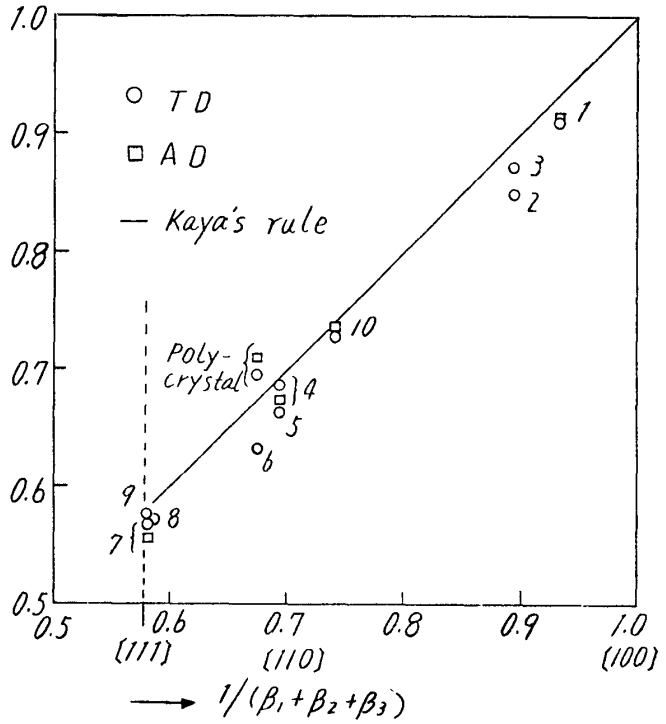

Fig. 6. Orientational dependence of the reduced "remanent" magnetization, I_k/I_s, in thermally demagnetized (TD) state (circles) and in alternating-current demagnetized (AD) state (squares) of 0.53% Al-Fe single crystals. The straight line expresses Kaya's rule $I_k/I_s = 1/(\beta_1+\beta_2+\beta_3)$.

axis, and thus the self-magnetic anneal effect by TD is not completely annihilated by the subsequent AD.

Finally, the measured I_k values for TD and for AD states of the polycrystal specimen are somewhat higher than the value computed by averaging simply Eq. (23) for all possible orientations[11]:

$$\overline{I_k} = I_s/\overline{\sum_{i=1}^{3}\beta_i} = 0.672\, I_s \tag{25}$$

(cf. Fig. 6). This fact, which has already been found with pure iron,[11] can be interpreted as due to the magnetic interaction between crystal grains or the tendency to reduce free magnetic poles distributing over grain boundaries.

XI. Coercive force

We have found that, in the limits of accuracy of our measurements, the measured values of the coercive force, H_c, which are independent of the demagnetizing factor, are not influenced by the method of demagnetization, irrespective of either for single crystals or for polycrystal, as seen from Table 2. Thus,

$$(H_c)_{TD} = (H_c)_{AD}\ . \tag{26}$$

Further, we see from Table 2 that in single crystal

$$H_{c\,[100]} < H_{c\,[110]} < H_{c\,[111]}\ , \tag{27}$$

and that

$$(H_c)_{poly} > (H_c)_{single} \ . \tag{28}$$

It is to be noted that the relation (27) has already been known to hold in the measured results of H_c in AD state of iron single crystals obtained by Kaya[11] (cf. Fig. 9 (a)), of 3.8% Si-Fe single crystals by Williams,[16] and of 1.2% Si-Fe single crystals by Tatsumoto[17] (cf. Fig. 9 (b)).

As was discussed in the introduction, the coercive force, H_c, can be considered to be essentially the critical field, H_o, of the 180° wall displacement. H_o is given by

$$H_0 = (\partial\gamma/\partial x)_{\max}/2I_s \cos\theta \ , \tag{29}$$

where γ and x are the energy and displacement of the 180° wall, respectively, and θ is the angle between the magnetization vector and the direction of magnetic field. $\partial\gamma/\partial x$ is generally changed by the method of demagnetization ; it is thought that its

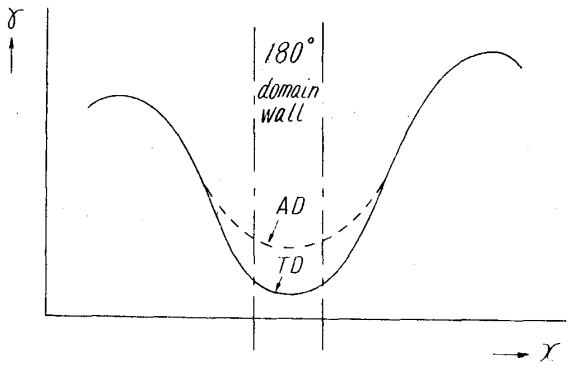

Fig. 7. Schematic representation of the effects of the thermal demagnetization (TD) and of the alternating current demagnetization (AD) on the positional variation of the 180° domain wall energy, γ.

value at the place where the 180° wall locates at unmagnetized state, $(\partial\gamma/\partial x)_o$, is larger in TD state than in AD state because of the self-magnetic anneal effect in the former state, but the value of $(\partial\gamma/\partial x)_{\max}$ which is associated with the place far distant from the 180° wall is hardly influenced by the method of demagnetization (cf. Fig. 7). Thus the observed relation (26) is explained.

Next, we consider, based on Kondorsky[18]-Vonsovsky's[19] theory, on the anisotropy of the coercive force. As mentioned in the introduction, 180° wall displacements occur exclusively as the magnetization is decreased from the break point of the descending hysteresis curve. Then, according to Kondorsky,[18] we have, for the coercive-force state ($I=0$, $H=H_c$), the following relations

(16) H. J. Williams : Phys. Rev., **52** (1939), 1004.
(17) E. Tatsumoto : J. Sci. Hiroshima Univ., **A16** (1952), 117.
(18) E. I. Kondorsky : C.R. Acad. Sci. USSR, **10** (1938), 397, 401.
(19) S. V. Vonsovsky : J. Phys. USSR, **11** (1940), 11.

$$2\,(I_s^2\,\chi_{/\!/}\sum_{i=1}^{3} v_{\bar{i}c}\,v_{ic}\,\beta_i^2)\,H_c = -\,I_s\ , \tag{30a}$$

and, when there is the grouping of 180° domains,

$$2\left\{I_s^2\,\chi_{/\!/}\sum_{i=1}^{3}\left(\frac{v_{ic}\,v_{\bar{i}c}}{v_{ic}+v_{\bar{i}c}}\right)\beta_i^2\right\}H_c = -\,I_s\ , \tag{30b}$$

where $\chi_{/\!/}$ is a constant, $i=1, \bar{1}, 2, \bar{2}, 3$, and $\bar{3}$ mean the [100], [$\bar{1}$00], [010], [0$\bar{1}$0], [001], and [00$\bar{1}$] directions, respectively, and v_{ic}'s are the relative volumes of domains magnetized along the i th direction. Now, since, as seen from the preceding section (X), the domain distribution at the break point of the descending hysteresis curve obeys approximately Kaya's rule,[11] the relative volumes of domains at this point, $v_{ik}(i,\ i=1, 2, 3)$, may be given by

$$v_{ik} = \beta_i/\sum_{j=1}^{8}\beta_j \quad\text{and}\quad v_{\bar{i}k} = 0 \quad (i, i, j = 1, 2, 3)\ . \tag{31}$$

Then, the relative volumes of domains in the coercive force state, v_{ic} $(i,\ \bar{i}=1, 2, 3)$, should be

$$v_{ic} = v_{\bar{i}c} = (1/2)\,\beta_i/\sum_{j=1}^{3}\beta_j \quad (i, j = 1, 2, 3)\ . \tag{32}$$

Substituting these values of v_{ic}'s and $v_{\bar{i}c}$'s into Eqs. (30a) and (30b), we have

$$H_c = H_{c\,[100]}\left\{\left(\sum_{i=1}\beta_i\right)^2/\sum_{i=1}^{3}\beta_i^4\right\} \tag{32a}$$

and, when there is the grouping of 180° domains,

$$H_c = H_{c\,[100]}\left(\sum_{i}\beta_i/\sum_{i=1}\beta_i^3\right)\ , \tag{32b}$$

where

$$H_{c\,[100]} = -\,2/\chi_{/\!/}\,I_s \tag{33}$$

According to Eqs. (32a) and (32b), the ratio of the H_c values for the [100], [110], [111] directions are

$$H_{c\,[100]} : H_{c\,[110]} : H_{c\,[111]} = 1 : 4 : 9\ , \tag{34a}$$

and, when there is the grouping of 180° domains,

$$H_{c\,[100]} : H_{c\,[110]} : H_{c\,[111]} = 1 : 2 : 3\ . \tag{34b}$$

The comparison of the measured H_c data with these formulae is shown in Fig. 8, which indicates that the measured data accords better to Eq. (32b) than to Eq. (32a). This shows that, irrespective of either in TD state or in AD state, the grouping of 180° domains predominantes in the coercive force state. It is to be noted that, the relation (32b) also holds in the results of measurements of the coercive force in AD state of iron single crystals by Kaya[11] (Fig. 9 (a)) and of

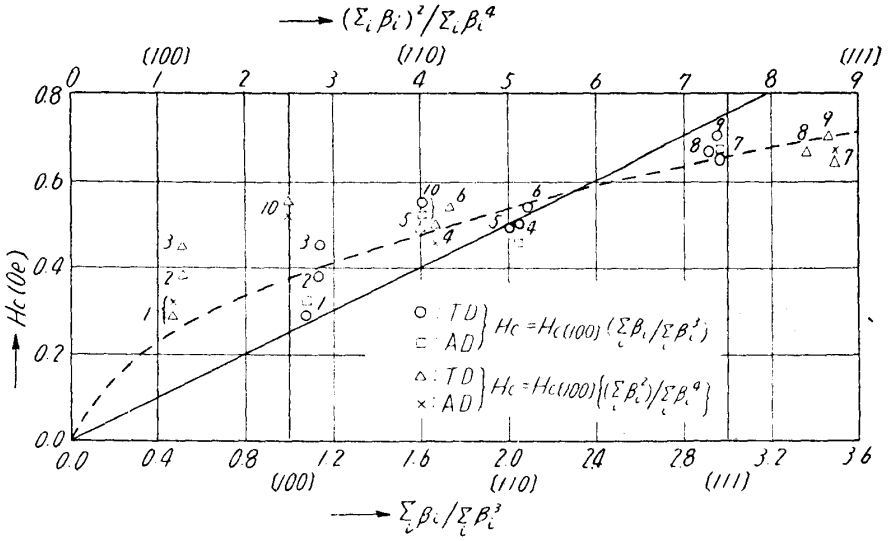

Fig. 8. Orientational dependence of the coercive force, H_c, in thermally demagnetized (TD) state and in alternating-current demagnetized (AD) state of 0.53% Al-Fe single crystals.

1.2% Si-Fe single crystals by Tatsumoto[17] (Fig. 9 (b)).

Finally, the relation (28), namely, that the coercive force of the polycrystal specimen is higher than those of single crystals of the same material has so far been observed frequently. This may be interpreted by the fact that the magnetic interaction between grains in the polycrystal makes the domain wall displacements difficult.

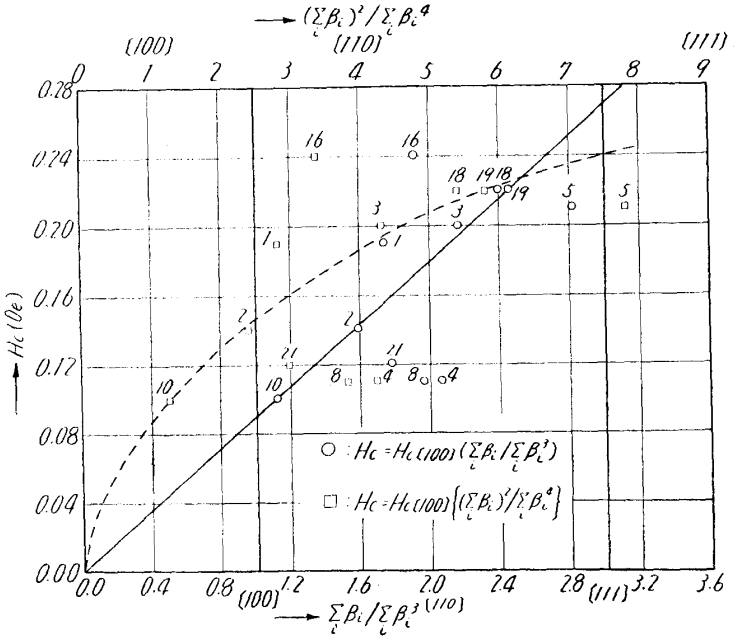

Fig. 9. (a)

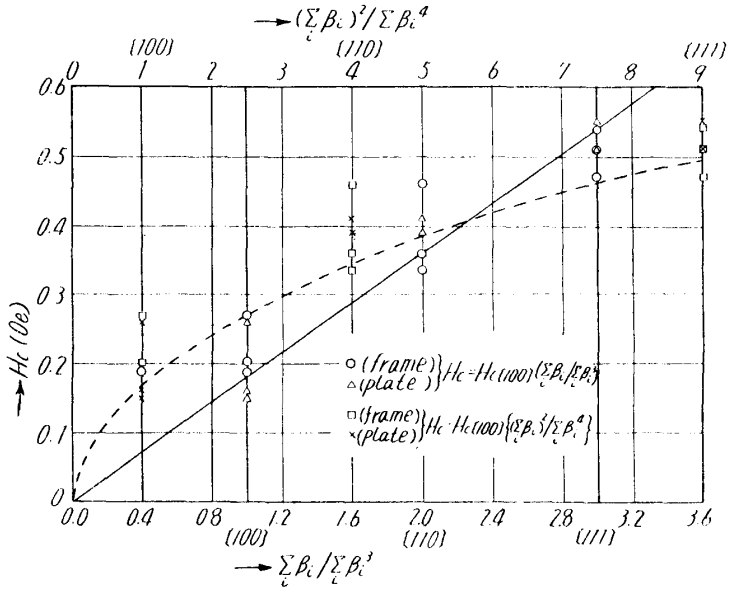

Fig. 9. (b)

Fig. 9. Orientational dependence of the coercive force, H_c, in alternating current demagnetized state of (a) iron single crystals (Kaya[2]) and of (b) 1.2% Si-Fe single crystals (Tatsumoto[4]).

XII. Initial magnetic susceptibility

We determined the values of the initial magnetic susceptibility, χ_0, from magnetization curves in weak field range (Fig. 10), which were measured

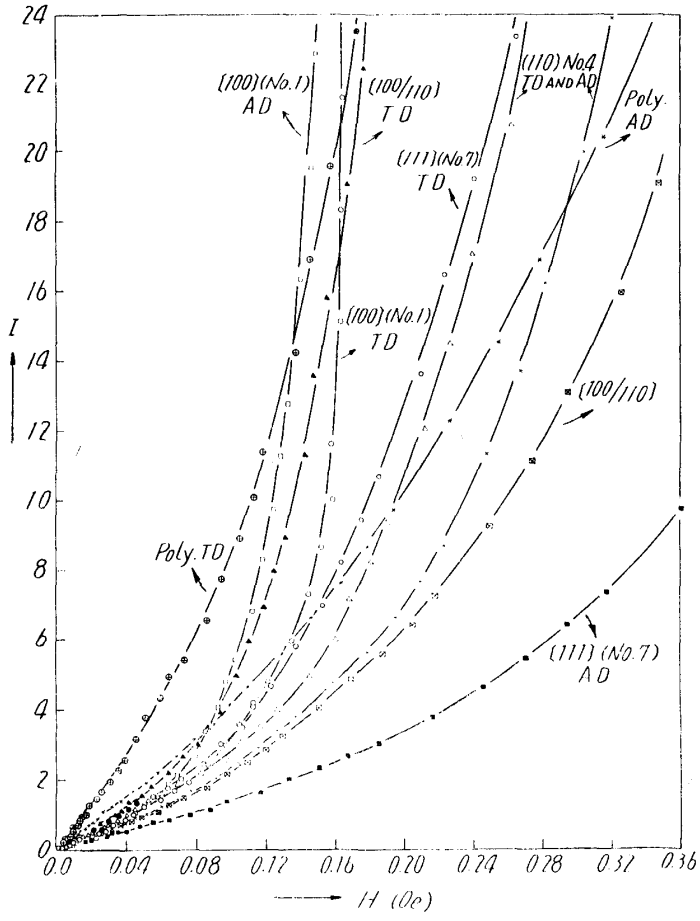

Fig. 10. Magnetization curves in very weak fields in thermally demagnetized (TD) state and in alternating-current demagnetized (AD) state of 0.53% Al-Fe single crystals and polycrystal.

separately from those described before in section VI. The measured χ_0 data are given in Table 2, which indicates the following facts :— Firstly, for single crystal specimens as well as for the polycrystal specimen,

$$(\chi_0)_{TD} > (\chi_0)_{AD} \ . \tag{35}$$

Secondly, for single crystal specimens, regardless of the method of demagnetization,

$$\chi_{0[100]} > \chi_{0[110]} > \chi_{0[111]} \ , \tag{36}$$

although the measured data are scattered to a considerable extent from specimen to specimen, and finally, irrespective of either in TD state or in AD state,

$$(\chi_0)_{poly} > (\chi_0)_{single} \ . \tag{37}$$

The relation (35) has already been found on iron single crystals[5,6,7] and iron, nickel, and 60 and 81.5% Ni-Fe polycrystals,[5] and the relation (36) has been observed on iron[11,5,6,7] (cf. Fig. 12 (a) and (b)) and 3.85% Si-Fe[16] (cf. Fig. 12 (c)) single crystals in AD state.

Now, according to the theory of the domain wall displacement as presented by Brown,[20] the change in relative volume, δv_i, by external force of the domain magnetized along the i th direction is given by

$$\delta v_i = \sum_{j \neq i} A_{ij} v_i v_j (u_j - u_i) \ , \tag{38}$$

where u_i is the free energy associated with the external force of the i domain and j means the direction of magnetization of a domain neighboring to the i domain. The factor A_{ij} is given by

$$A_{ij} = a \, . \, \overline{\left[\partial \left\{(w_i - w_j) + (\partial\gamma/\partial x_{ij})_0\right\}/\partial x_{ij}\right]^{-1}} \ , \tag{39}$$

where w_i is the free energy associated with the internal stress of the i domain, γ the domain wall energy, x_{ij} the positional coordinate of the ij domain wall, and — means the average. The factor a is generally given by

$$a = S_{ij}/v_i v_j \ , \tag{40a}$$

or, when 180° domains are grouped, by

$$a = S_{i\bar{i}} \cdot (v_i + v_{\bar{i}})/v_i v_{\bar{i}} \ . \tag{40b}$$

In the case of the present study, the external force is the magnetic field, H,applied along a direction whose direction cosines are $(\beta_1, \beta_2, \beta_3)$ and the directions of magnetization in domains are six $\langle 100 \rangle$ directions since the cubic ferromagnetic anisotropy constant, K_1, is positive. Therefore,

$$u_i = -HI_s\beta_i \text{ and } u_{\bar{i}} = HI_s\beta_i \ . \tag{41}$$

Here, we assume that A_{ij}'s for 180° walls are all equal to A and those for 90° walls are all equal to B, and we put

(20) W. F. Brown : Phys. Rev., **55** (1939), 568.

$$\alpha = AI_s \text{ and } \beta = BI_s \ . \tag{42}$$

and also

$$x_i = v_i + v_{\bar{i}} \text{ and } \quad y_i = v_i - v_{\bar{i}} \ , \tag{43}$$

so that

$$\sum_i x_i = 1 \text{ and } \sum_i \beta_i y_i = j = I/I_s \ , \tag{44}$$

where I is the magnetization of the specimen as a whole. Then, we get, from Eq. (38),

$$\delta x_i = \beta \left(\beta_i y_i \sum_{j \neq i} x_j - x_i \sum_{j \neq i} \beta_j y_j\right) \delta_H \tag{45}$$

and

$$\delta y_i = \left\{\alpha\beta_i (x_i^2 - y_i^2) + \beta \left(\beta_i x_i \sum_{j \neq i} x_j - y_i \sum_{j \neq i} \beta_j y_j\right)\right\} \delta_H \ , \tag{46a}$$

or, when 180° domains are grouped

$$\delta y_i = \left\{\alpha \beta_i (x_i^2 - y_i^2)/x_i + \beta \left(\beta_i x_i \sum_{j \neq i} x_j - y_i \sum_{j \neq i} \beta_j y_j\right)\right\} \delta H \ . \tag{46b}$$

Thus, we have, from Eqs. (44) and (46a) or (46b),

$$\delta j/\delta H = \alpha \sum_i \beta_i^2 (x_i^2 - y_i^2) + \beta \sum_i \left(\beta_i^2 x_i \sum_{j \neq i} x_j - \beta_i y_i \sum_{j \neq i} \beta_j y_j\right) \ , \tag{47a}$$

or, when 180° domains are grouped,

$$\delta j/\delta H = \alpha \sum_i \{\beta_i^2 (x_i^2 - y_i^2)/x_i\} + \beta \sum_i \left(\beta_i^2 x_i \sum_{j \neq i} x_j - \beta_i y_i \sum_{j \neq i} \beta_j y_j\right) \ . \tag{47b}$$

If we denote the relative volume of domains in the unmagnetized state as v_{io}'s ($i=\bar{1}$, 1, 2, $\bar{2}$, 3, and $\bar{3}$), then, $v_{io}=v_{\bar{i}o}$, and, consequently, $x_{io}=2v_{io}$ and $y_{io}=0$. Thus, the initial magnetic susceptibility, χ_0, as defined by

$$\chi_0 = (\delta j/\delta H)_0 I_s \ , \tag{48}$$

is given, from Eq. (47a), by

$$\chi_0 = 2 I_s \sum_i \beta_i^2 v_{i0} \left\{2 (\alpha - \beta) v_{i0} + \beta\right\} \tag{49a}$$

and, from Eq. (47b), by

$$\chi_0 = 2 I_s \sum_i \beta_i^2 v_{i0} (\alpha + \beta - 2 \beta v_{i0}) \ . \tag{49b}$$

Here, we consider two extreme cases regarding α and β. The first is the case where $\alpha=\beta=AI_s$, which is valid for statistical domain theory,[20] and the second is the case where $\beta=0$, namely, only 180° wall displacements contribute to the initial susceptibility, which is valid, needless to say, only for the case where all of 180° domains are grouped. For the former case, we get, from Eqs. (49a) and (49b),

$$\chi_0 = 2 A I_s^2 \sum_i \beta_i^2 v_{i0} \tag{50a}$$

and

$$\chi_0 = 4AI_s^2 \sum_i \beta_i^2 v_{i0}(1-v_{i0}) \ , \tag{50b}$$

respectively, and, for the latter case, we get, from Eq. (49b), Eq. (50b) again. Further, if we assume that the domain distribution in the unmagnetized state is given, just as in the coercive-force state ($I=0$, $H=H_c$) (cf. Section XI), by

$$v_{i0} = v_{j0}, \ (1/2)\,\beta_i / \sum_{j=1}^{3} \beta_j \qquad (i, j = 1, 2, 3) \ , \tag{51}$$

then we get, from Eqs. (50a) and (50b),

$$\chi_0 = \chi_{0\,[100]} \left(\sum_i \beta_i^3 / \sum_i \beta_i \right) \tag{52a}$$

and

$$\chi_0 = \chi_{0\,[100]} \left\{ 2 \cdot \frac{\sum_i \beta_i^3}{\sum_i \beta_i} - \frac{\sum_i \beta_i^4}{(\sum_i \beta_i)^2} \right\} , \tag{52b}$$

respectively, where

$$\chi_{0\,[100]} = AI_s^2. \tag{53}$$

Eqs. (52a) and (52b) give, as the ratio of the initial susceptibilities along the [100], [110], and [111] directions,

$$\chi_{0\,[100]} : \chi_{0\,[110]} : \chi_{0\,[111]} = 1 : 1/2 : 1/3 \tag{54a}$$

and

$$\chi_{0\,[100]} : \chi_{0\,[110]} : \chi_{0\,[111]} = 1 : 3/4 : 5/9 \ , \tag{54b}$$

respectively.

These expressions are compared with the measured data in Fig. 11, which indicates that Eqs. (52a) and (52b) accords equally well with the measured data. Then, it follows that, for our 0.53% Al-Fe single crystals in TD state as well as in AD state, (1) there is no grouping of 180° domains, and 180° and 90° wall displacements contribute equally to the initial susceptibility, or (2) there is the grouping of 180° domains, and 180° and 90° wall displacements contribute equally or only 180° wall displacements contribute to the initial susceptibility. But, the before-described consideration on the anisotropy of the coercive force has indicated that there is the grouping of 180° domains in our 0.53% Al-Fe single crystals and the magnetostriction measurements, which will be reported in a separate paper, shows that only 180° wall displacements contribute to the initial susceptibility in our single crystals. Thus, Eq. (52b) is taken as the expression for the anisotropy of the initial susceptibility in our 0.53% Al-Fe single crystals.

It is to be noted, further, that Kaya's[11] measured data on $(\chi_0)_{AD}$ of iron single crystals are expressed better by Eq. (52a) than by Eq. (52b), as shown in Fig. 12(a). Shimizu's[5] measured data on $(\chi_0)_{TD}$ of iron single crystals are also expressed well by Eq. (52b), but his measured data on $(\chi_0)_{AD}$ are fitted better to

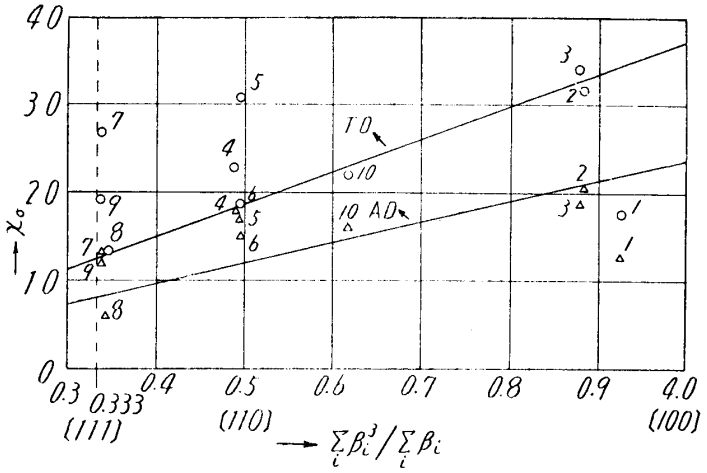

Fig. 11. (a) χ_0 as dependent on $\sum_i \beta_i^3 / \sum_i \beta_i$

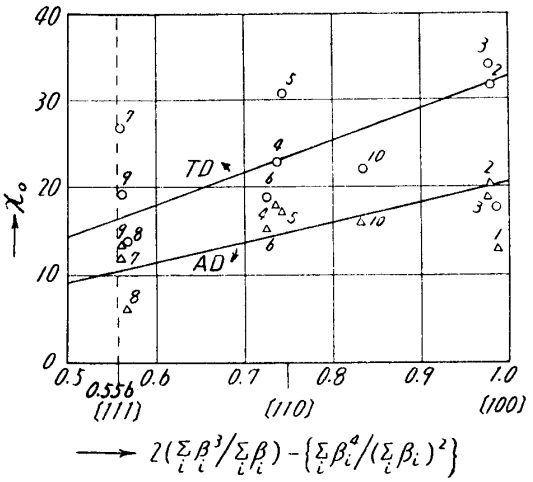

Fig. 11. (b) χ_0 as dependent on $2 \cdot \dfrac{\sum_i \beta_i^3}{\sum_i \beta_i} - \dfrac{\sum_i \beta_i^4}{\left(\sum_i \beta_i\right)^2}$

Fig. 11. Orientational dependence of the initial magnetic susceptibility, χ_0, in thermally demagnetized (TD) state (circles) and in alternating-current demagnetized (AD) state (triangles) of 0.53% Al-Fe single crystals.

Eq. (52b) than Eq. (52a), as may be seen from Fig. 12(b). Tomono's[7] measured data on $(\chi_0)_{TD}$ and on $(\chi_0)_{AD}$ of iron single crystal are expressed well by Eq. (52b) and by Eq. (52a), respectively. William's[16] measured data on $(\chi_0)_{AD}$ of 3.85% Si-Fe single crystals are in a better accordance with Eq. (52a), as shown in Fig. 12(c). In short, the anisotorpy of χ_0 in iron and silicon iron crystals with $K_1>0$ is expressed by Eq. (52a) or (52b). It should be noticed, however, that this holds for the anisotropy of χ_0 at ordinary temperatures. Shimizu[5] has shown that the anisotropy of $(\chi_0)_{AD}$ in iron single crystals varies with rising temperature in such a way that $\chi_{0[100]} : \chi_{0[110]} : \chi_{0[111]}$ changes from 1 : 1/2 : 1/3 at −170°C through 1 : 3/4 : 5/9 at ordinary temperature to 1 : 1 : 1 just below the Curie temperature. Thus, it may be said that the anisotropy of $(\chi_0)_{AD}$ in iron single crystals obeys Eq. (52a) at lower temperatures where K_1 is larger, but, at ordinary tem-

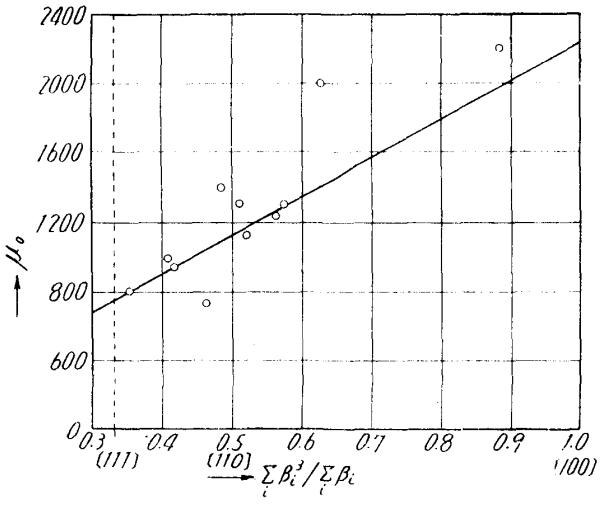

(a) Fe single crystals in alternating-current demagnetized state(Kaya[11])

(b) Fe single crystals in thermally magnetized state (circles) and in alternating-current demagnetized state (triangles) (Shimizu[5])

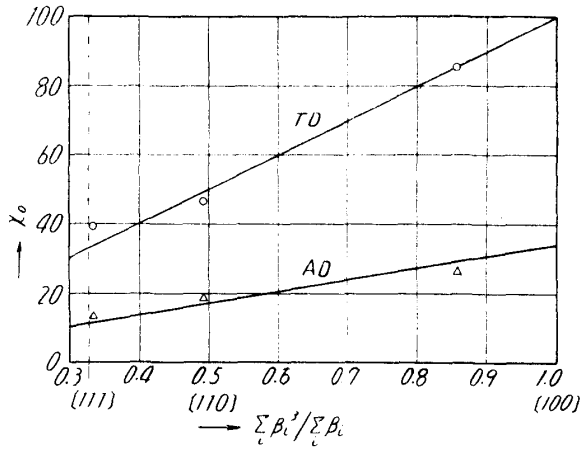

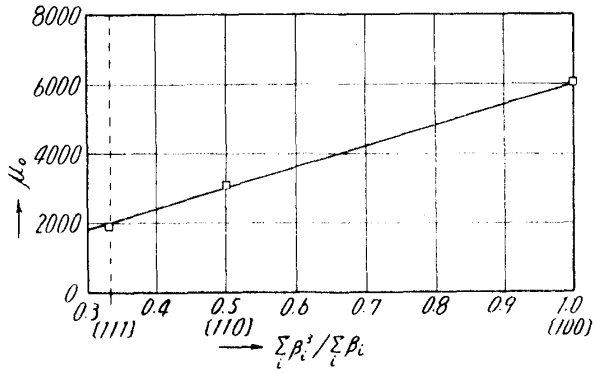

(c) 3.85% Si-Fe single crystals (picture-frame specimens) in alternating-current demagnetized state (Williams[16])

Fig. 12. Orientational dependence of the initial magnetic permeability, μ_0, or susceptibility, $\chi_0(\sim\mu_0/4\pi)$

peratures where K_1 is moderate, it obeys Eq. (52b), and finally, at higher temperatures where K_1 vanishes, it naturally becomes isotropic.

As mentioned above, if only 180° wall displacement contributes to χ_0,

$$\alpha = AI_s \quad \text{and} \quad \beta = BI_s = 0 \ , \tag{55}$$

and, according to Eq. (39),

$$A = A_{i\bar{i}} = a \cdot \overline{\left[\partial \left\{(w_i - w) + (\partial \gamma/\partial x_{i\bar{i}})_0\right\}/\partial x_{i\bar{i}}\right]^{-1}} , \tag{56}$$

which is rewritten as

$$A = a \cdot \overline{\left\{\text{const.} + (\partial^2 \gamma/\partial x_{i\bar{i}}{}^2{}_0\right\}^{-1}} , \tag{57}$$

since w_i–$w_{\bar{i}}$ or the term of the free energies associated with internal stress in Eq. (56) can be considered as unaffected by the method of demagnetization. Now, as discussed in the preceding section, $(\partial\gamma/\partial x_{i\bar{i}})_0$ and hence $(\partial^2\gamma/\partial x^2{}_{i\bar{i}})_0$ may be larger in TD state than in AD state because of the self-magnetic-anneal effect in the former state (cf. Fig. 7). Then, Eq. (57) indicates that, if a is constant, then $A_{TD} < A_{AD}$, so that $(\chi_{0[100]})_{TD} < (\chi_{0[100]})_{AD}$ according to Eq. (53), and hence, generally, $(\chi_0)_{TD} < (\chi_0)_{AD}$, which is inconsistent with the observed relation (35). On the other hand, however, a is given by Eq. (40b) in this case and the volumes of individual domains, v_i, may be smaller and hence the surface areas of domain walls, $S_{i\bar{i}}$, may be larger in TD state than in AD state, so that

$$a_{TD} > a_{AD} . \tag{58}$$

Then, even if $[(\partial^2\gamma/\partial x^2{}_{i\bar{i}})_0]_{TD} < [(\partial^2\gamma/\partial x^2{}_{i\bar{i}})_0]_{AD}$ as mentioned above, when the value of the constant or $\partial(w_i - w_{\bar{i}})/\partial x_{i\bar{i}}$ in Eq. (56) is sufficiently large, it becomes that

$$A_{TD} > A_{AD} , \tag{59}$$

and hence $(\chi_0)_{TD} > (\chi_0)_{AD}$, which is consistent with the observational fact (35).

Although it is considered that $[(\partial^2\gamma/\partial x^2{}_{i\bar{i}})_0]_{TD} < [(\partial^2\gamma/\partial x^2{}_{i\bar{i}})_0]_{AD}$, as stated above, these $\partial^2\gamma/\partial x^2{}_{i\bar{i}}$ values may be lower than the ones observed usually with pure iron owing to the self-magnetic-anneal effect by TD on the one hand and owing to the locking of domain walls by interstitial impurity atoms after AD on the other hand. This may be the reason for the fact that χ_0 in 0.53% Al-Fe alloys is generally lower than in pure iron.

Further, similarly to the above interpretation of the observed relation $(\chi_0)_{TD} > (\chi_0)_{AD}$, it is considered that, in the polycrystal specimen, the volumes of domains are smaller and hence the surface areas of domain walls are larger because of the existence of grain boundaries in it, so that $a_{poly} > a_{single}$ and hence $(\chi_0)_{poly} > (\chi_0)_{single}$, regardless of the value of $\partial^2\gamma/\partial x_{i\bar{i}}$ and of the method of demagnetization.

Finally, it is to be noted that, since, in any single crystal specimen as well as in the polycrystal specimen, $(\chi_0)_{TD} > (\chi_0)_{AD}$, as stated above, and $(H_s)_{TD} > (H_s)_{AD}$, as stated in Section IX, TD and AD magnetization curves cross with each other.